Title
Effect of Heating Rate on Sintering and Coarsening

Journal
Journal of the American Ceramic Society, 76(6)

Authors
Jonghe, L.C. De
Rahaman, M.N.
Chu, M.-Y.

Publication Date
1989-06-01

LBL-26823
Preprint

Center for Advanced Materials

CAM

Submitted to Journal of the American Ceramic Society

Effect of Heating Rate on Sintering and Coarsening

L.C. De Jonghe, M.N. Rahaman, and M.-Y. Chu

June 1989

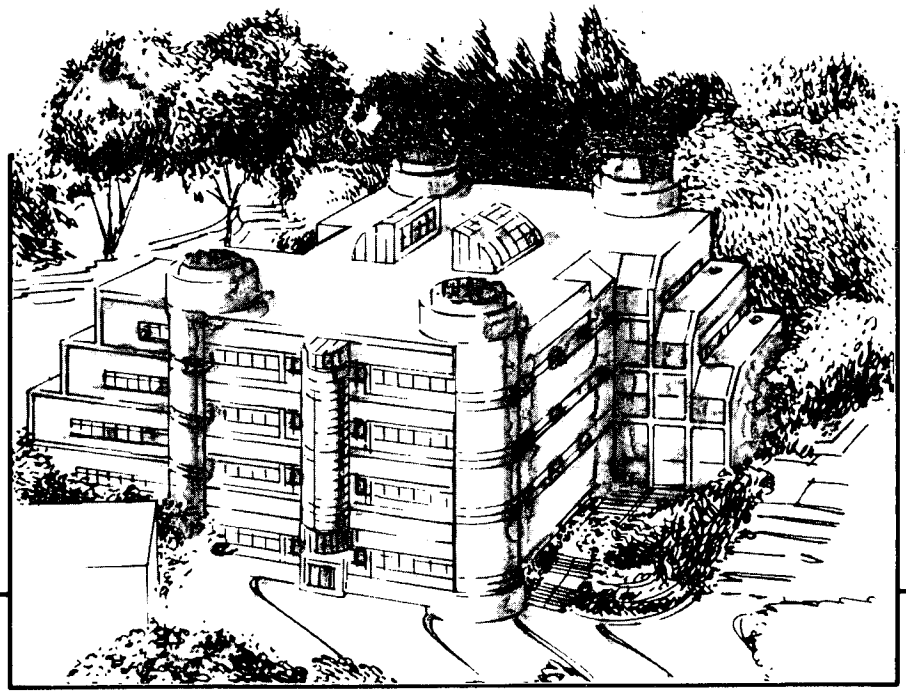

Materials and Chemical Sciences Division

Lawrence Berkeley Laboratory • University of California

ONE CYCLOTRON ROAD, BERKELEY, CA 94720 • (415) 486-4755

Prepared for the U.S. Department of Energy under Contract DE-AC03-76SF00098

DISCLAIMER

LBL # 26823

EFFECT OF HEATING RATE ON SINTERING AND COARSENING

Lutgard C. De Jonghe* ***, Mohamed N. Rahaman* **, and May-Ying Chu* ***

Center for Advanced Materials

Materials and Chemical Sciences Division

Lawrence Berkeley Laboratory

One Cyclotron Road

University of California, Berkeley, CA 94720

and Richard J. Brook

Max-Planck Institut für Metallforschung

Heisenbergtrasse 5, D-7000 Stuttgart 80, West Germany

Supported by the Division of Materials Sciences, Office of Basic Energy Sciences, U.S. Department of Energy, under Contract No. DE-AC03-76SF00098

* Member, the American Ceramic Society

** Permanent address: The University of Missouri-Rolla, Department of Ceramic Engineering, Rolla, Missouri 65401

*** Also with the Department of Materials Science and Engineering, University of California, Berkeley, CA 94720

Abstract

The sintering of zinc oxide power compacts has been investigated at constant rates of heating of 0.5 - 15°C/min. For samples with the same initial relative density (0.50), the temperature derivative of the densification strain versus density fits a common curve. At low temperatures the densification rate as a function of temperature increases almost linearly with the heating rate. The data, covering a wide density range of 0.5 - 0.98, are consistent with an analysis that accounts for the coarsening (defined as an increase in the mean pore separation) in terms of two classes of microstructural coarsening processes: those associated respectively with densifying and with non-densifying mechanisms.

I. INTRODUCTION

An important processing goal for technical ceramics is obtaining a uniform microstructure, at high density with desired grain size. To obtain this goal a range of experimental techniques, such as hot pressing or varying the time-temperature schedule of the sintering process, are available. In this paper the effects of particular time-temperature schedules, constant heating rate sintering, are examined. Such non-isothermal processing steps are quite important since they occur, to varying degrees of approximation, in all sintering processes. Even the so-called isothermal sintering has a heat-up period in which considerable microstructural development and densification can occur; frequently, more than half of the possible densification of a ceramic compact is reached at the end of this heat-up phase, regardless of how rapidly it is executed. In several instances, very rapid heating, also called fast firing, has produced beneficial effects in maintaining relatively fine microstructures at high sintered densities.[1,2] The heating rate is thus an intrinsic part of sintering, either used as a parameter to influence the course of microstructural evolution or as a contribution to the starting conditions for conventional, constant-temperature processing.

Much work on the effect of heating rate on sintering was conducted fifteen to twenty years ago. Typically, data for the initial stage sintering of amorphous or polycrystalline powder compacts were correlated with data obtained under isothermal sintering conditions. Only limited success was achieved for polycrystalline systems. This was primarily due to the difficulties in analyzing sintering data when several transport mechanisms were active simultaneously. Cutler[3] studied the initial sintering of spherical glass powder compacts at constant rates of heating from 0.4-2.9°C/min and compared

the data with the predictions of Frenkel's model.[4] Good agreement between theory and experiment was obtained if the viscosity of the glass was described by a thermally activated process with a fixed activation energy. The initial stage sintering of polycrystalline powder compacts has been studied by Young and Cutler[5] who analyzed their data in terms of an equation developed by Johnson[6] for the sintering of two spherical particles by simultaneous volume, grain-boundary, and surface diffusion. Young and Cutler suggested that, in constant heating rate experiments, there may be distinct temperature regions in which grain-boundary or volume diffusion may dominate over surface diffusion. This behavior was, however, not readily apparent from the data. Woolfrey and Bannister[7] formulated techniques for analyzing the initial stage shrinkage during constant heating rate sintering and concluded that, in principle, their techniques permit the determination of all the sintering parameters normally obtained from isothermal sintering data. Data for the rate law, diffusion coefficient, and activation energy obtained from constant heating rate and isothermal sintering of UO_2 and ThO_2 showed good agreement. Woolfrey and Bannister's results might be considered to be fortuitous since, as in the work of Young and Cutler,[5] a central issue, i.e. the simultaneous occurrence of more than one sintering mechanism was not addressed.

Recently, Lange[8] studied the sintering of Al_2O_3 powder compacts with the same initial density at constant rates of heating of 2.5-20°C/min up to 1500°C. For each heating rate, the shrinkage strain rate increased to a maximum and then decreased. The maximum densification strain rate occurred at approximately the same relative density of 0.77 for each heating rate. Lange suggested that sintering kinetics dominated the densification process up to a relative density of 0.77 after which coarsening kinetics dominated. In contrast to the earlier work discussed above that studied the initial stage of sintering only,

the data of Lange covered almost the entire densification process. It is interesting to note here that the maximum densification rate occurred at densities where under isothermal conditions logarithmic densification is observed.

It is frequently documented and generally accepted that the critical issue in microstructure development is the interplay between densification and coarsening. Usually coarsening is described by the evolution of grain size. While for dense materials this is undoubtedly the feature of importance, model-based descriptions of densification rates must be based on the mean interpore separation. A convenient assumption is to put the grain size about equal to the pore separation, but a microstructural examination of most partly-sintered compacts reveals that this is not a very accurate assumption. With respect to the densification rates, it is proposed that the relevant coarsening parameter is the *increase in the mean pore-separation*, X. With this definition, and with a distribution of pore sizes in a given matrix, two classes of processes can be recognized as contributing to coarsening: non-densifying processes, such as ones governed by surface diffusion and evaporation/ condensation, and densifying process, such as the ones brought about by the disappearance of the smaller pores in the distribution as a consequence of densification. It must then be expected, if the temperature dependence of these two classes of coarsening mechanisms are considered, that at least two different activation energies should be needed to describe the temperature dependence of coarsening. One objective of the paper is to show the influence of the heating rate under conditions where the two coarsening processes are effective.

Earlier work by De Jonghe and coworkers[9,10] indicated that ZnO and CdO can be useful as model oxides for isothermal sintering studies. It should again be

noted that logarithmic densification was observed up to at least .92 of the theoretical density. It was found for these, as well as for a number of other ceramics and glasses, that the ratio of the densification rate to the constant-stress creep rate, from the onset of densification to sintered densities in excess of 0.9 of theoretical remains constant. For ZnO[10], this constancy of the ratio was also observed under conditions of a constant heating rate of 4°C/min. Subsequent experiments following the same procedures with heating rates of 2°C/min and 8°C/min also showed a constant ratio of the densification rate to the constant stress creep rate (Fig. 1). This leads to the conclusion that the sintering stress, which is related to this ratio, is likely to be constant under similar conditions. The present paper examines the non-isothermal densification behavior of ZnO powder compacts at constant heating rates between 0.5 and 15°C/min. All compacts had the same initial density of 0.50±0.01 of theoretical, and the experiments were terminated at 1100°C when the sample reached relative densities in excess of 0.96 of theoretical. The analysis, using relatively simple and model unspecific rate expressions, predicts qualitatively the major effects of the densification behavior, such as the insensitivity of both the densification strain and the temperature derivative of the densification strain to the heating rate. In addition, the analysis shows the need to include separate coarsening processes with different activation energies to account for the data obtained at various heating rates.

II. EXPERIMENTAL PROCEDURE

ZnO powder compacts (6mm diameter by 6mm) of the same initial density (0.50 ± 0.01 of theoretical) were made by uniaxial compression of the powder at ~20 MPa in a tungsten carbide die. Constant heating rate sintering was performed in a dilatometer at five imposed heating rates ranging from 0.5 to

15°C/min. The same procedure was used in all sintering runs; the sample was heated at 10°C/min from room temperature to 500°C (below which temperature no densification could be detected) followed by a controlled heating rate to 1100°C, after which the sample was cooled rapidly. The shrinkage of a standard quartz sample was measured under identical conditions in order to correct for differences in shrinkage between the dilatometer* push rod and the sample holder. The density of the ZnO sample was determined from its initial density and the measured shrinkage. The microstructure of selected samples was observed by scanning electron microscopy of fracture surfaces.

III. RESULTS

Figure 2 shows results for the relative density, ρ, vs. temperature, T. For samples with the same green density of 0.50 $\pm$ 0.01 and sintered at constant rates of heating ranging from 0.5 to 15°C/min. The data for any heating rate are reproducible to within $\pm$1%. The curves have the familiar sigmoidal shape and, generally, are shifted to higher temperatures with increasing heating rate; the final densities are high (0.96-0.98). It can be noted that the achieved sintered densities at any temperature showed a systematic, although not very pronounced dependency on the heating rates.

The temperatures derivative of the densification strain, $(1/\rho)d\rho/dT$, is plotted in Fig. 3 as a function of temperature for the different heating rates. Each curve increases to a maximum and then decreases; the maximum shifts slightly but systematically to higher temperatures as the heating rate increases.

*Harrop Industries, Inc., Columbus, OH

Figure 4 shows the data for $(1/\rho)d\rho/dT$ plotted as a function of ρ. The data fit a common curve for the relatively wide range of heating rates used. Much higher heating rates could not be used with the existing equipment; in addition, higher heating rates can be expected to lead to problems with thermal gradients in the sample. Much lower heating rates are very time-consuming and difficult to control accurately.

Figure 5 shows the data for the densification strain rate, $(1/\rho)d\rho/dt$, plotted as a function of temperature for the heating rates used. The maximum of the curves shifts slightly to higher temperature with increasing heating rate. Above ~700°C the densification strain rate at a fixed temperature increases approximately linearly with heating rate; however, below this temperature the increase in densification rate is lower. It can also be noted that in the early stages of sintering (~550°C) the densification strain rate is not independent of heating rate; moreover, if the curves are extrapolated to 500°C (at which temperature measurable shrinkage begins) they do not converge to a single densification strain rate.

Scanning electron micrographs of fracture surfaces of samples sintered at constant heating rates of 15°C/min (referred to as sample A) and 0.5°C/min (sample B) are shown in Fig. 6(a) and (b), respectively; both samples were heated to 1100°C and then cooled. Sample A shows a uniform, equiaxed microstructure with an average grain size of 4μm. The grain size of the ZnO starting powder was 0.1-0.4 μm. The microstructure of sample B is less uniform and there appears to be appreciable trans-granular fracture; the average grain size of the sample is ~10 μm.

IV. DISCUSSION

Model

A striking feature of the data is that the temperature derivative of the densification strain, $(1/\rho)d\rho/dT$, plotted as a function of density, Fig. 4, fits a common curve for the wide range of heating rates used (Fig. 4). Similar data have been obtained recently by Lange[8] for Al_2O_3 powders. The Al_2O_3 data also showed that the shrinkage strain rate increased to a maximum at $\rho = 0.77$ and then decreased, from which Lange concluded that the sintering kinetics controlled densification below $\rho = 0.77$ after which coarsening kinetics dominated. As seen from Fig. 4, the present data for ZnO do not show a sharp maximum at $\rho = 0.77$; instead a relatively constant, plateau region between ρ values of 0.60 and 0.80 is observed.

As a first step in the analysis, it is instructive to determine how well the present ZnO data can be explained by existing sintering models. Rahaman and De Jonghe[9] showed that the densification strain rate of the same ZnO powder under isothermal conditions followed a relationship based on a Nabarro-Herring model[11,12] for volume-diffusion controlled densification strain rate, $\dot{\epsilon}$, i.e.,

$$\dot{\epsilon} = (1/\rho)\ d\rho/dt = H\ D\ \Sigma\ \phi^{3/2}/\ (X^2kT) \qquad \text{Eqn. 1*}$$

where ρ is the instantaneous density, H is a geometrical factor, D is the volume diffusion coefficient, Σ is the sintering stress[13], ϕ is the stress

*In previous publications the sintering stress was either denoted as Σ or as Σ/ϕ; for uniformity the symbol Σ is now adopted for the sintering stress.

intensification factor [18,13], X is an average interpore distance, k is the Boltzmann factor, and T is the absolute temperature. The sintering stress, Σ, has also been referred to as the sintering force[14], the sintering potential[15], or the sintering pressure.[16] The mean boundary stress for free sintering is $\Sigma\phi$. The term ϕ is of geometrical origin[17,18], and is akin to the efficiency factor introduced by DeHoff[19].

Equation 1 is generally held to describe adequately only the early stages of sintering, but recent work by Chu et al.[10], using the same ZnO powder, has indicated that it is applicable over a much wider range of sintered densities: from the onset of densification to as high as 0.92 of theoretical density. Within the same range, it could be inferred from the constancy of the densification rate over the constant-stress creep rate that the sintering stress, Σ, was nearly constant for any given specimen, even under conditions of constant heating rate[10]. Thus, the sintering stress in Eqn. 1 may be regarded, with some confidence, as a constant when interpreting the data.

If the sintering stress is constant, then the only terms in Eqn. 1 that can explain the change in the densification strain rate are the microstructural terms, X, the average interpore spacing; and the scale insensitive factor, ϕ. In general the assumption is made that if a pore is present on each corner of the grain then the pore spacing is approximately equivalent to the grain size. Therefore the grain size is frequently substituted for X. For simplicity a microstructural factor, M, including both X and ϕ will be used, to describe the combined effects of X and ϕ.

The general observation of logarithmic densification during isothermal sintering is

$$\rho \propto t^{m} \qquad \text{Eqn. 2}$$

where ρ is the instantaneous density, t is the time, or the equivalent

$$\Delta\epsilon \propto \log(t) \qquad \text{Eqn. 3}$$

and $\Delta\epsilon$ is the densification strain

This well-documented experimental observation requires that

$$\dot{\epsilon} \propto 1/t \qquad \text{Eqn. 4}$$

For Eqn. 1 to conform to the commonly observed isothermal logarithmic densification the microstructural factor M must therefore be in the form of

$$M^{n} = M_{o}^{n} + C.t \qquad \text{Eqn. 5}$$

where M_o is the initial microstructural pore spacing, n is an integer that depends on the transport mechanism, and C is a constant, in view of the constancy of Σ, H, and D at constant T. Note that the expression for $M^n(t)$, Eqn. 5, has the same format as the usual grain-growth relationships.

Under non-isothermal conditions, Eqn. 1 can still be used if it is modified to take into account the temperature dependence of the coarsening factor, M(T,t), and of the diffusion coefficient, D:

$$\dot{\epsilon} = [1/\rho]d\rho/dt = K\ D(T)\ /[\ M^{n}(T,t)]\ kT \qquad \text{Eqn. 6}$$

where $K = H\ \Sigma$ and $M^n = X^n/\phi^{(n+1)/2}$ (n depends on the transport mechanism). It will

assumed, as discussed before, that Σ is a constant, so that K is also a constant. D(T) is the diffusion coefficient for the densifying transport mechanism:

$$D(T) = D_o \exp(-Q_d/kT) \qquad \text{Eqn. 7}$$

where D_o is a constant and Q_d is the activation energy associated with densification. Equation 5 may be rewritten as

$$M^n = M_o^n + C(T).t \qquad \text{Eqn.8}$$

where M_o, is the initial microstructural parameter at $t=t_o$, and C(T)t is the coarsening function, with

$$C(T) = C_o \exp(-Q_c/kT) \qquad \text{Eqn. 9}$$

C_o is a constant, and Q_c is the activation energy associated with coarsening.

At high density, when the stress intensification factor ϕ approaches 1, M becomes equivalent to the pore spacing, X. At lower densities, however, $M = X/\phi^{(n+1)/2n}$, becomes significantly smaller than the mean pore spacing. In any system the mean pore spacing will increase when a pore disappears. The removal of a pore can be accomplished by either densifying mechanisms, or by non-densifying mechanisms. These two processes are distinct and are likely to have different activation energies and different relative importance at different sintering stages. Processes with low activation energies must dominate at the low temperatures and conversely processes with high activation energies will be dominant at the higher temperatures. Since constant heating rate experiments sample a wide temperature range the coarsening function will

be more appropriately described by including two temperature dependent components:one relating to densifying processes, and the other relating to non-densifying processes. Eqn. 8 is therefore rewritten as

$$M^n = M_o^n + A(T).t + B(T).t \qquad \text{Eqn. 10}$$

A(T)t is associated with densifying mechanisms,

$$A(T) = A_o \exp(-Q_d/kT) \qquad \text{Eqn. 11}$$

where A_o is a constant, while B(T)t is associated with non-densifying mechanisms,

$$B(T) = B_o \exp(-Q_{nd}/kT) \qquad \text{Eqn. 12}$$

where B_o is a constant, Q_{nd} is the activation energy associated with the non-densifying processes, and n is characteristic of the transport mechanism. In principle, more than one term of this type would need to be included; for the present, however, only one dominant term for non-densifying mechanisms will be considered sufficient.

The expression of Eqn. 10 rests on the assumption that coarsening rates are simply additive; it is, at present, not based on a detailed micromechanistic analysis of the transport processes involved but has the merit of conforming, under isothermal conditions, to the form of the usual coarsening expression. Eqn. 10 also asumes that the effects of the various transport mechanisms on coarsening are simpply additive. Clearly, this assertion will require further study. For now, it is examined how well the expression serves in analyzing the data. Eqn. 10 expresses clearly the dependence of the coarsening

on the two different classes of transport processes. The constants A_o and B_o will determine the relative importance of the two processes. Typically, it should be expected that an activation energy for non-densifying coarsening, Q_{nd}, would be significantly lower than Q_d, when these processes involve surface transport in a continuous pore network. A general statement can, however, not be made, and actual values are likely to be system specific.

For non-isothermal conditions, where the temperature changes with time, as in the case of constant heating rate experiments, Eqn. 10 can be written as

$$M^n(T,t) = M_o^n + A_o\int_0^t \exp(-Q_d/kT)dt + B_o\int_0^t \exp(-Q_{nd}/kT)dt \quad \text{Eqn. 13}$$

In constant heating rate experiments, for which $T = T_o + \alpha t$, with α as the heating rate, the increment of time, dt, is related to the temperature increment, dT through α, i.e.

$$dt = dT/\alpha \quad \text{Eqn. 14}$$

Then Eqn. 13 becomes

$$M^n(T,t) = M_o^n + (A_o/\alpha)\int_{T_o}^{T} \exp[-Q_d/(kT)]dT + (B_o/\alpha)\int_{T_o}^{T} \exp[-Q_{nd}/(kT)]dT \quad \text{Eqn. 15}$$

Limiting cases of no coarsening and extreme coarsening

a. no coarsening

The limiting cases, of extreme coarsening and no coarsening, can be examined using Eqns. 6 and 15. First, consider the case where little or no coarsening is observed, $M = M_o$, so $\dot{\epsilon}$ is independent of α, then upon integration, at a given temperature, $T = T_o + \alpha t$:

$$\Delta\epsilon = \int_{t_o}^{t} \dot{\epsilon} dt \qquad \text{Eqn. 16}$$

or

$$\Delta\epsilon = (1/\alpha)\int_{T_o}^{T} \dot{\epsilon} dT \qquad \text{Eqn. 17}$$

so the incremental densification strain at a fixed temperature is *inversely proportional* to the heating rate. This means that at a given temperature, T, the density of the sample with the slower heating rate will be higher than for the sample with a faster heating rate.

b. extreme coarsening

In the other extreme, where significant coarsening has occurred:

$$M_o^{\,n} << A_o \int \exp(-Q_d/kT)dt + B_o \int \exp(-Q_{nd}/kT)dt \qquad \text{Eqn. 18}$$

Now Eqn. 6 can be written as

$$\dot{\epsilon} = \alpha[K.D(T)]/[A_o\int(\exp(-Q_d/kT))dT + B_o\int(\exp(-Q_{nd}/kT))dT] \qquad \text{Eqn. 19}$$

here $\dot{\epsilon}$ at a given temperature depends both on that temperature and the heating rate, α. Upon integration, $\Delta\epsilon$, at a given temperature is seen to be *independent* of the heating rate and depends only on the temperature.

It can be noted that the precise form of the coarsening relationship is actually not important in obtaining the dependence of the sintered strain increment $\Delta\epsilon$ on the heating rate for constant heating rate sintering. For $M >> M_o$, M^n can be expressed in a general form, conforming to logarithmic

densification, as

$$M^n \propto \int f(T)dt \qquad \text{Eqn. 20}$$

and the same conclusions would follow: when $M \gg M_o$, the densification strain is only dependent on the temperature and is independent of the heating rate, α. This is simply a consequence of the system following isothermal logarithmic densification kinetics, when C in Eqn. 8 is some function of temperature only.

More generally, if the coarsening relationship, for constant heating rate α Eqn. 15 would be approximated by

$$M^n = \alpha^{-u} f(T) \qquad \text{Eqn. 21}$$

the densification strain rate, $\dot{\epsilon}$, becomes:

$$\dot{\epsilon} = \alpha^{u} F(T) \qquad \text{Eqn. 22}$$

The parameter u ranges from 0 for very fast heating rates ($M \approx M_o$) to 1 for very slow heating rates ($M \ggg M_o$). Numerical calculations, using some reasonable values for the various activation energies, readily show that Eqn. 22 is an adequate approximation of Eqns. 6 and 13, with a maximum error of about 20 percent, within about one decade of heating rates. In other words, extrapolations ranging over about one decade of heating rates around a particular heating rate experiment may be made with u constant, when u has been determined for that heating rate.

From Eqn. 22 it follows immediately for the temperature derivative of the

densification strain, $d\epsilon/dT$, that

$$d\epsilon/dT = \alpha^{u-1}F(T) \qquad \text{Eqn. 23}$$

and for the incremental densification strain, $\Delta\epsilon$, that

$$\Delta\epsilon = \alpha^{u-1}\int F(T)dT \qquad \text{Eqn. 24}$$

so that a plot of the temperature derivative of the densification strain, $d\epsilon/dT$, versus the incremental sintered density, $\Delta\rho$, will again be independent of the heating rate, at least over a range of heating rates of about one decade, even if $M \gg M_o$ is not satisfied. In practice, since Eqn. 21 is only an approximation, some dependence on the heating rate will remain. This is quite consistent with the data shown in Fig. 4.

Coarsening versus non-coarsening

It is interesting to contrast the expected consequences of heating rate on systems that do not coarsen (e.g. monosize particles) and systems that do coarsen. As evident in Eqn. 17, when coarsening is absent or minimal then at a specific temperature, the incremental strain, $\Delta\epsilon$, should depend inversely on the heating rate. This has, in fact, been observed for a near monomodal system of TiO_2 by Barringer et al.[20]. The relationship is shown in Fig. 7, in which some of the data obtained by Barringer et al. have been replotted to show the incremental shrinkage as a function of heating rate, at a fixed temperature of 1156 °C. At the highest shrinkage, at a $\Delta l/l_o = 0.15$, the corresponding density is about 0.9 of theoretical, and little coarsening was observed. For the present ZnO system, in which coarsening is significant, the densification strain rate at a low temperature should be proportional to the

heating rate, as indicated by Eqn. 19. This behavior is shown in Fig. 8. For higher heating rates, where coarsening is less pronounced, it is expected that deviation from this relationship will be apparent.

In ultra-rapid firing or fast firing, where approximately constant high heating rates are used and where the final density depends mostly on the temperature reached, Johnson[2] pointed out that this process is very effective for small particle powders. Due to the high ratio of surface area to volume, coarsening is increasingly difficult to suppress for compacts of particles with decreasing average size, and it should be expected that for submicron, non-monosized powders the condition $M >> M_o$ is likely to be established as soon as densification is significant. As the discussion here indicates, under this condition $\Delta\rho$ just depends on the temperature and is independent of the heating rate. This particular characteristic of fast firing, according to this analysis, resides in the use of fine particles which coarsens easily rather than in avoiding coarsening while dwelling at low temperatures.

Numerical calculations

The complexity of the expressions for the dependence of the densification strain rate, $\dot{\epsilon}$, on temperature, even in the experimental limits of low and high temperature, precludes a straightforward extraction of meaningful activation energies from the data. In the case of negligible coarsening, as expected with large or monosize particles at high heating rates, it should be observed that $\dot{\epsilon}$ at a given temperature is independent of the heating rate. At that point the activation energy for diffusional transport can be obtained with some confidence from the low-temperature region of the constant heating rate data. In other cases the qualitative profiles of the densification strain rate versus temperature can be reproduced by numerically integrating Eqns. 6

and 15 and adjusting the values of the various constants.

Assuming only one coarsening process to be active, the one associated with densifying processes and characterized by Q_d, Eqns. 6 and 15 will predict a densification behavior as shown qualitatively in Fig. 9. This plot was generated by using Q_d = 50 kcal/mol, with values for the prefactors and M_o^n such that M^n at 600°C is equal to twice M_o^n. The densification strain rate at heating rates of 10°C/min and 2°C/min will be initially independent of the heating rate, α, as long as little coarsening has occurred. When coarsening starts to become significant, the densification rate reaches a maximum, and then decreases in spite of the increasing temperature.

The maximum densification strain rate increases with increasing heating rate. On the one hand, it must be noted that computations assuming a single activation energy for coarsening, Q_c, as in Eqn. 8, do not lead to a maximum in the densification strain rate if Q_d-Q_c is larger than ≈ 5kcal/mol. If Q_c-Q_d is larger than ≈ 5kcal/mol, on the other hand, the densification strain rate decreases monotonically with increasing temperature, a behavior that is clearly contrary to normal sintering behavior. The profile of the densification strain rate versus temperature for various conditions using a single activation energy for coarsening is shown in Fig. 10. If the prefactor C(T) in Eqn. 8 is chosen such that coarsening dominates at low temperatures, with $Q_c \approx Q_d$ then a large pore spacing would develop rapidly with increasing temperature, causing a maximum in the densification rate close to the onset of densification. The major feature of the ZnO data, Fig. 4 and Fig. 5, is that the densification strain rates are proportional to the heating rate at the onset of observable densification, while showing a clear maximum under conditions where Eqns. 10 or 13 still should be valid. This behavior cannot be described using only one activation energy for coarsening.

A low temperature coarsening process, such as associated with a non-densifying mechanism with an activation energy, Q_{nd}, lower than Q_d, as described in Eqn. 15, must be included in the calculation to conform, even qualitatively, to the experimental results. The calculated behavior, shown in Figure 11, approximating well the observed densification behavior of ZnO under constant heating rate, was generated using Q_{nd} = 15 kcal/mol and Q_d = 50 kcal/mol, with the prefactors and M_o^n such that M^n at 525°C is twice M_o^n.

It may therefore be concluded that the description of the coarsening process in ZnO, under constant heating rate conditions is consistent with a coarsening process, i.e., an evolution of the mean interpore spacing, that has two components: a low temperature one of low activation energy, operating while the densification rate is very low, and thus associated with *non-densifying* processes, and a *coarsening* mechanism operating at high temperatures, with an activation energy comparable to that of densification and therefore associated with densifying mechanisms. It is the latter that causes the densification rate to decrease before the final density is reached.

While the experimental examinations are limited here to ZnO, it is plausible that similar processes of coarsening, characterizable by contributions of densifying and non-densifying processes in coarsening, may be recognized in most real non-isothermal sintering of ceramic powder compacts.

SUMMARY

The significance of coarsening for sintering is best revealed when the process is defined as an increase in the mean pore separation. Analysis of the constant heating rate conditions can then be performed using a modified

isothermal densification rate equation to account for the changes in the microstructural spacing as a function of time and temperature. The modification consists in recognizing that for a sample with a distribution of pore sizes there are contributions of densifying and non-densifying processes to coarsening.

For non-coarsening, where $M_o = M(T,t)$, the modified rate equation predicts that the densification strain rate is, at a given temperature independent of the heating rate, α, and that the incremental strain, $\Delta\epsilon$, at a given temperature is proportional to α^{-1}. This result is corroborated by the sintering behavior of monosized particles.

For significant coarsening, where $M \gg M_o$, the modified rate equation predicts the densification strain rate, at a given temperature to be proportional to the heating rate, α, while the incremental strain, $\Delta\epsilon$, is only dependent on the temperature.

The sintering of ZnO at various heating rates shows results consistent with the case where coarsening is significant from the onset of sintering. The densification strain rate behavior with respect to temperature is consistent with a coarsening process characterized by two types of activation energies, one attributed to densifying processes at higher temperatures and the other to non-densifying processes at lower temperatures.

Figures

Fig. 1. Axial strain versus radial strain for ZnO: 2°C/min (circle), 4°C/min (square), and 8°C/min (filled square).

Fig. 2. Relative density versus temperature for ZnO powder compacts with the same green density (0.50 ± 0.01) and sintered at constant rates of heating shown (in °C/min).

Fig. 3. Change in densification strain per unit change in temperature as a function of temperature calculated from Fig. 1.

Fig. 4. Change in densification strain per unit change in temperature as a function of density calculated from Fig. 1.

Fig. 5. Densification strain rate versus temperature calculated from Fig. 1.

Fig. 6. Scanning electron micrographs of fracture surfaces of samples sintered to 1100°C at constant heating rates of (a) 15°C/min. and (b) 0.5°C/min.

Fig. 7. Log of the heating rate^{-1} versus log of the incremental shrinkage at a constant temperature of 1156°C [20].

Fig. 8. Densification strain rate versus heating rate, evaluated at 600°C.

Fig. 9. Densification strain rate versus temperature calculated from Eqns. 6 and 15 with heating rates of 10°C/min and 2°C/min using the activation energy of 50 kcal/mol for both densification and coarsening. M_o^n and prefactors were chosen such that $M^n = 2M_o^n$ at 600°C for the heating rate at 2°C/min.

Fig. 10. Densification strain rate versus temperature calculated from Eqns. 6 and 15 with a heating rate of 4°C/min using an activation energy for densification of 50 kcal/mol, and activation energies for coarsening of 50 kcal/mol, 45 kcal/mol, or 40 kcal/mol. M_o^n and prefactors were chosen such that $M^n = 2M_o^n$ at 600°C for the activation energy of coarsening at 50 kcal/mol.

Fig. 11. Densification strain rate versus temperature calculated from Eqns. 6 and 15 with heating rates of 10°C/min and 2°C/min using activation energies for densification as 50 kcal/mol, and activation energies for coarsening as 50 kcal/mol and 15 kcal/mol. M_o^n and prefactors were chosen such that $M^n = 2X_o^n$ at 525°C for the heating rate at 2°C/min.

Reference

1. R. J. Brook, "Fabrication Principles for the Production of Ceramics with Superior Mechanical Properties," *Proc. Brit. Ceram. Soc.*, 32 7 (1982).

2. D. L. Johnson, "Ultra-Rapid Sintering", *Materials Science Research Vol. 16*, ed. G. C. Kuczynski, A. E. Miller and G. A. Sargent (Plenum Press, New York, 1984) p.243.

3. I. B. Cutler, "Sintering of Glass Powders During Constant Rates of Heating," *J. Am. Ceram. Soc.*, 52 [1] 14 (1969).

4. J. Frenkel, "Viscous Flow of Crystalline Bodies Under the Action of Surface Tension," *J. Phys. (USSR)*, 9 [5] 385 (1945).

5. W. S. Young and I. B. Cutler, "Initial Sintering with Constant Rates of Heating," *J. Am. Ceram. Soc.*, 53 [12] 659 (1970).

6. D. L. Johnson, "New Method of Obtaining Volume, Grain-Boundary, and Surface Diffusion Coefficients from Sintering Data," *J. Appl. Phys.*, 40 [1] 192 (1969).

7. J. L. Woolfrey and M. J. Bannister, "Nonisothermal Techniques for Studying Initial-Stage Sintering." *J. Am. Ceram. Soc.*, 55 [8] 390 (1972).

8. F. F. Lange, "Approach To Reliable Powder Processing" *Ceramic Transactions*, 1, 1069 (1989).

9. M. N. Rahaman, L. C. De Jonghe, "Creep-Sintering of Zinc Oxide," *J. Mater. Sci.*, 22 4326 (1987).

10. M.-Y. Chu, L. C. De Jonghe, and M. N. Rahaman, "Effect of Temperature on the Densification/Creep Viscosity During Sintering," *Acta. metall.* 37 [5] 1415 (1989).

11. F. R. N. Nabarro, "Deformation of Crystals by the Motion of Single Ions"; p. 75 in Report on the Conference of Strength of Solids, Bristol, England, 1947, 1948.

12. C. Herring, "Diffusional Viscosity of a Polycrystalline Solid," *J. Appl. Phys.*, 21 [5] 437 (1950).

13. L. C. De Jonghe and M. N. Rahaman, "Sintering Stress of Homogeneous and Heterogeneous Powder Compacts," *Acta metall.* 36 [1] 223 (1988).

14. F. N. Rhines and R. T. DeHoff "Sintering and Heterogeneous Catalysis", *Materials Science Research Vol. 16*, ed. by G. C. Kuczynski, A. E. Miller and G. A. Sargent (Plenum Press, New York, 1984) p.49.

15. C. H. Hsueh, A. G. Evans, R. M. Cannon, and R. J. Brook, "Viscoelastic Stresses and Sintering Damage in Heterogeneous Powder Compacts," *Acta metall.*, 34 [5] 927 (1986).

16. R. Raj and R. K. Bordia, "Sintering and Behavior of Bimodal Compacts," *Acta metall.*, 32 [7] 1003 (1984).

17. W. Beeré, "A Unifying theory of the Stability of Penetrating liquid Phases and Sintering Pores," *Acta metall.* 23 [1] 131 (1975).

18. W. Beeré, "The Second Stage Sintering Kinetics of Powder Compacts," *Acta metall.* 23 [1] 139 (1975).

19. R. T. DeHoff, "A Cell Model for Microstructural Evolution during Sintering", *Materials Science Research Vol. 16*, ed. G. C. Kuczynski, A. E. Miller and G. A. Sargent (Plenum Press, New York, 1984) p.49.

20. E. A. Barringer, R. Brook, and H. K. Bowen, "The Sintering of Monodisperse TiO_2" *Materials Science Research Vol. 16*, ed. G. C. Kuczynski, A. E. Miller, G. A. Sargent (Plenum Press, New York 1984) p. 1.

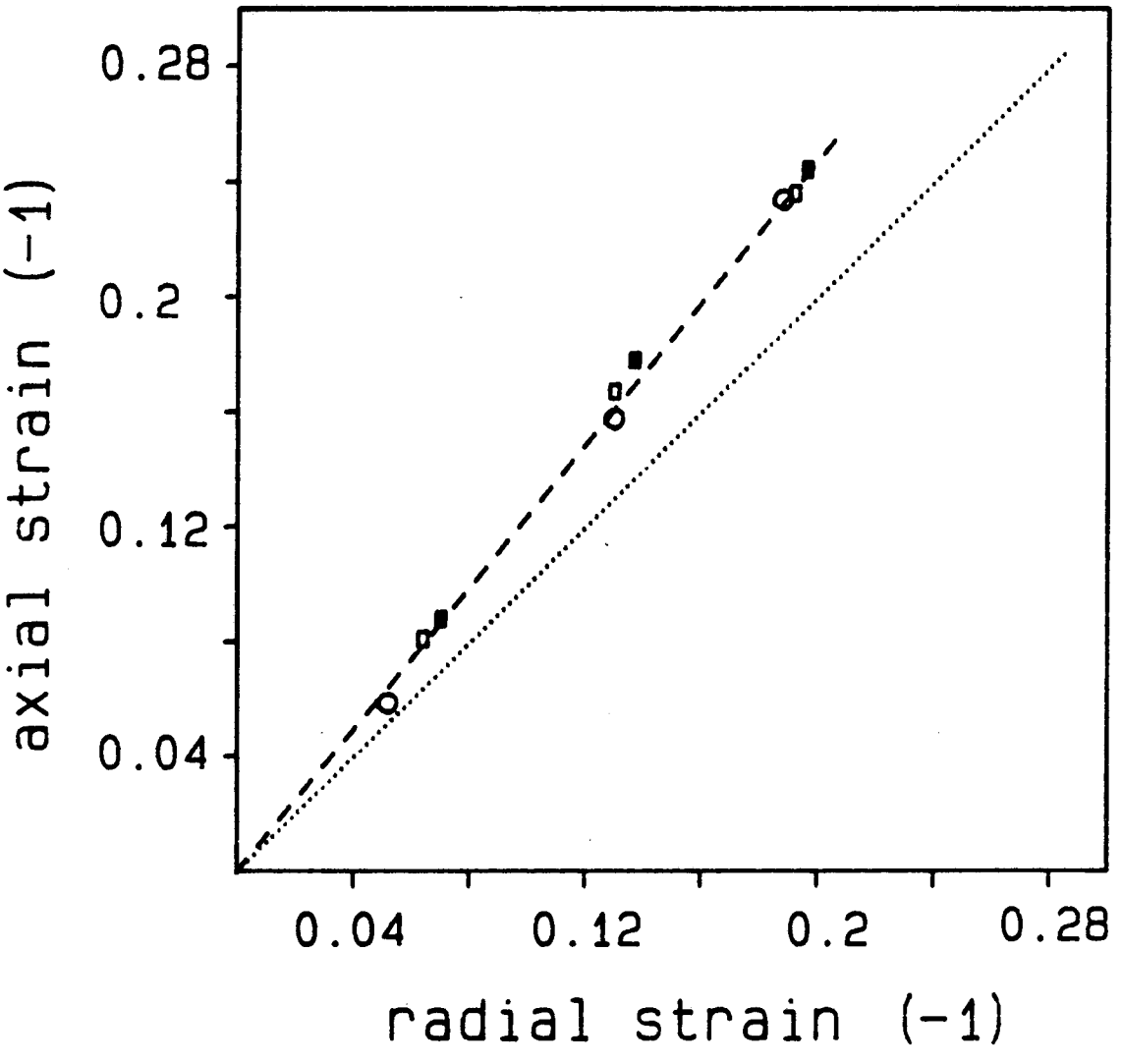

XBL 896-2386

Figure 1

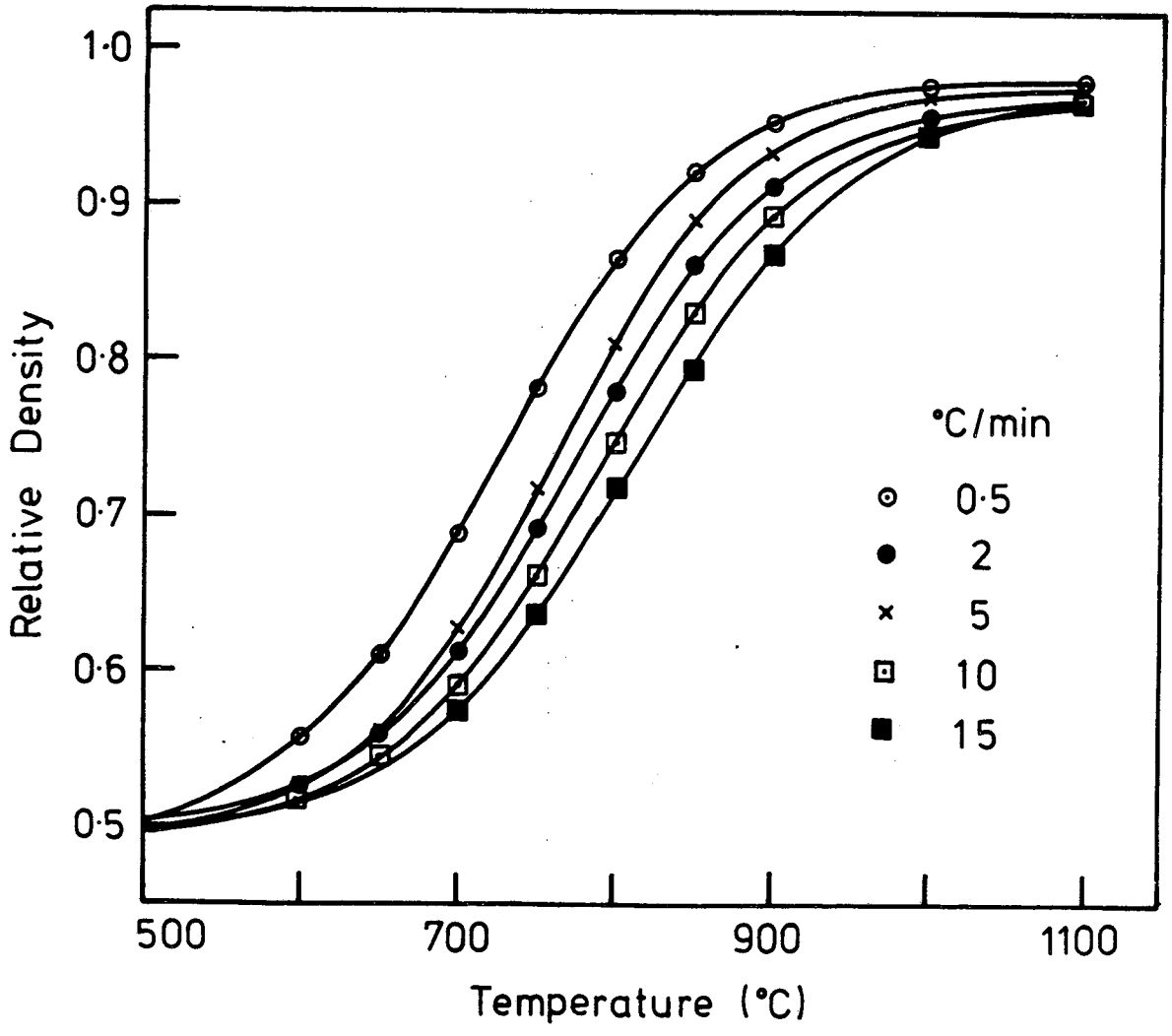

XBL 893-902

Figure 2

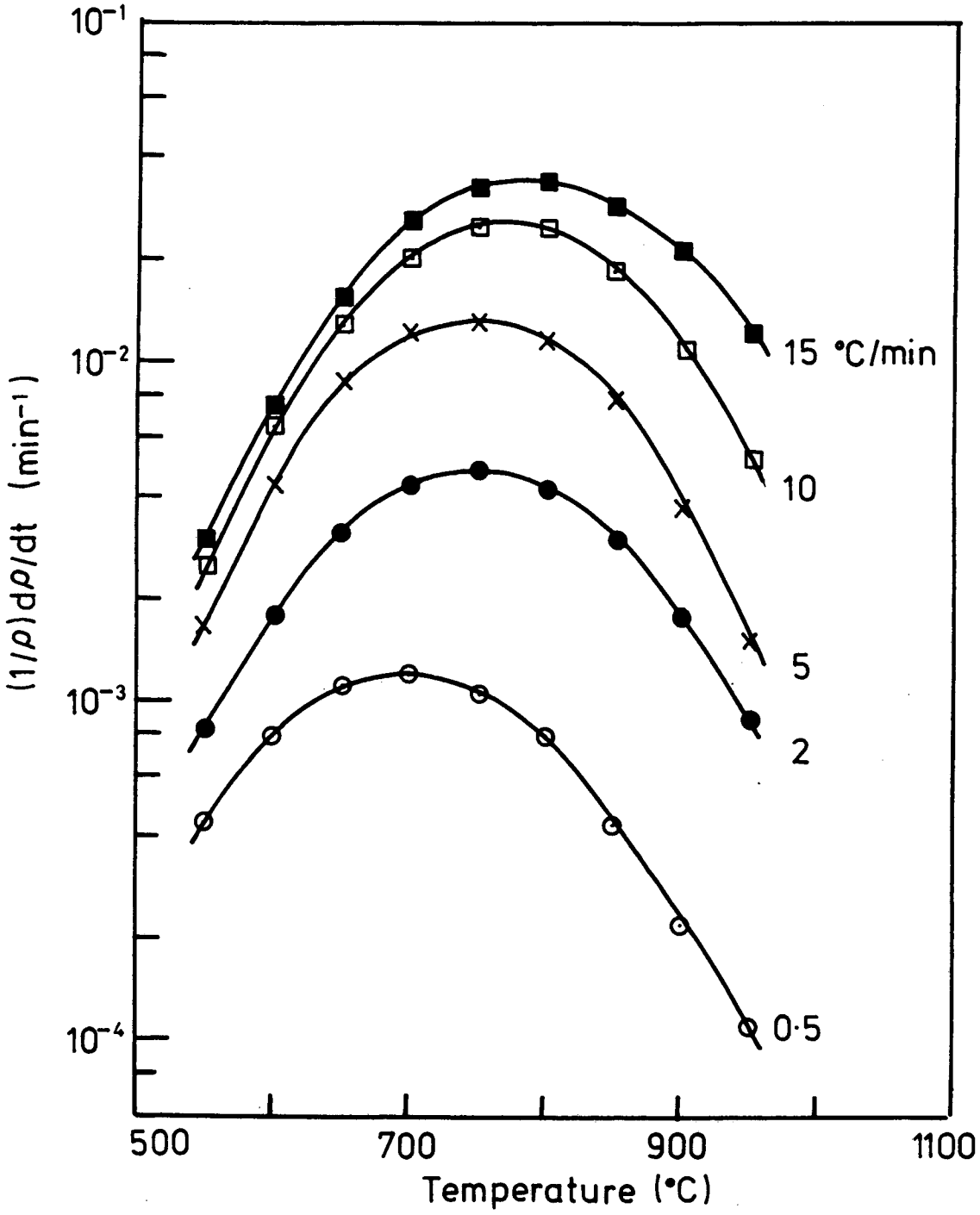

XBL 893-905

Figure 3

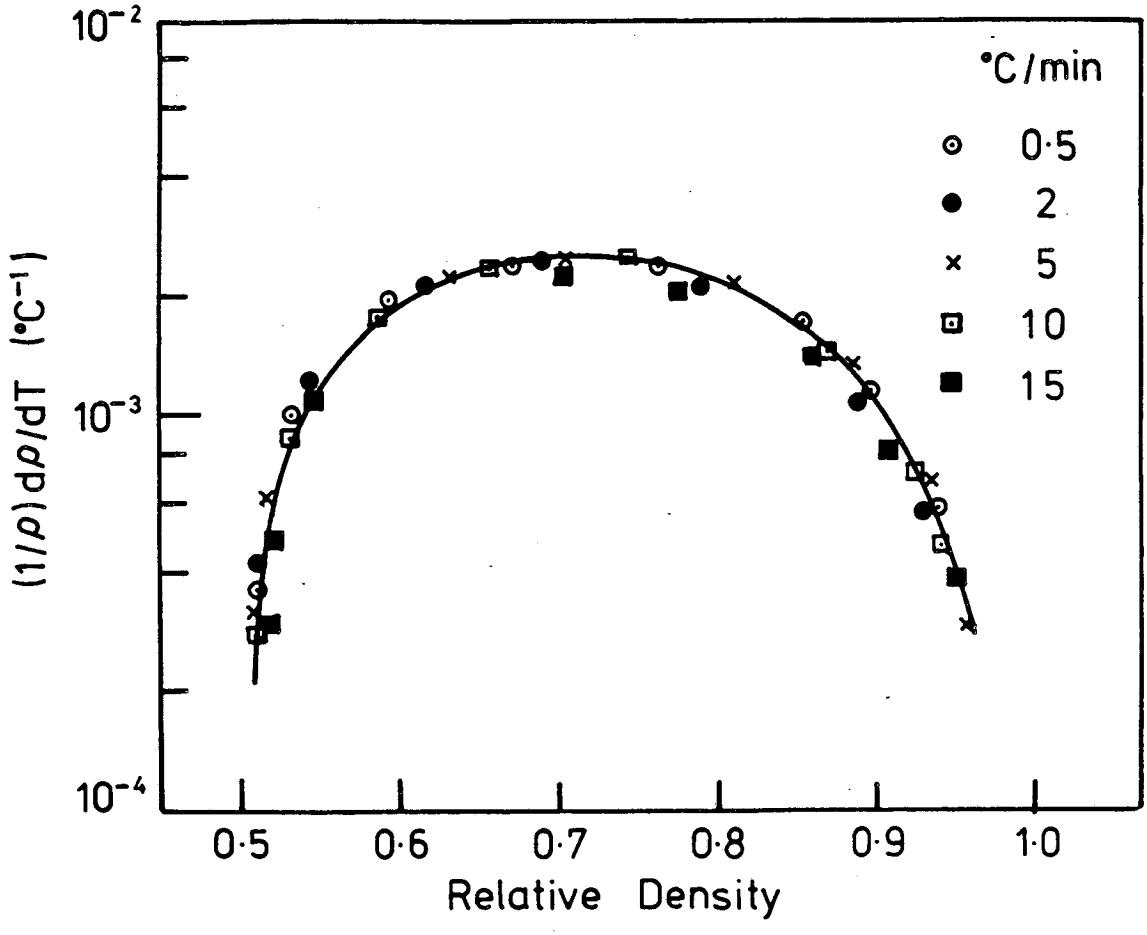

XBL 893-904

Figure 4

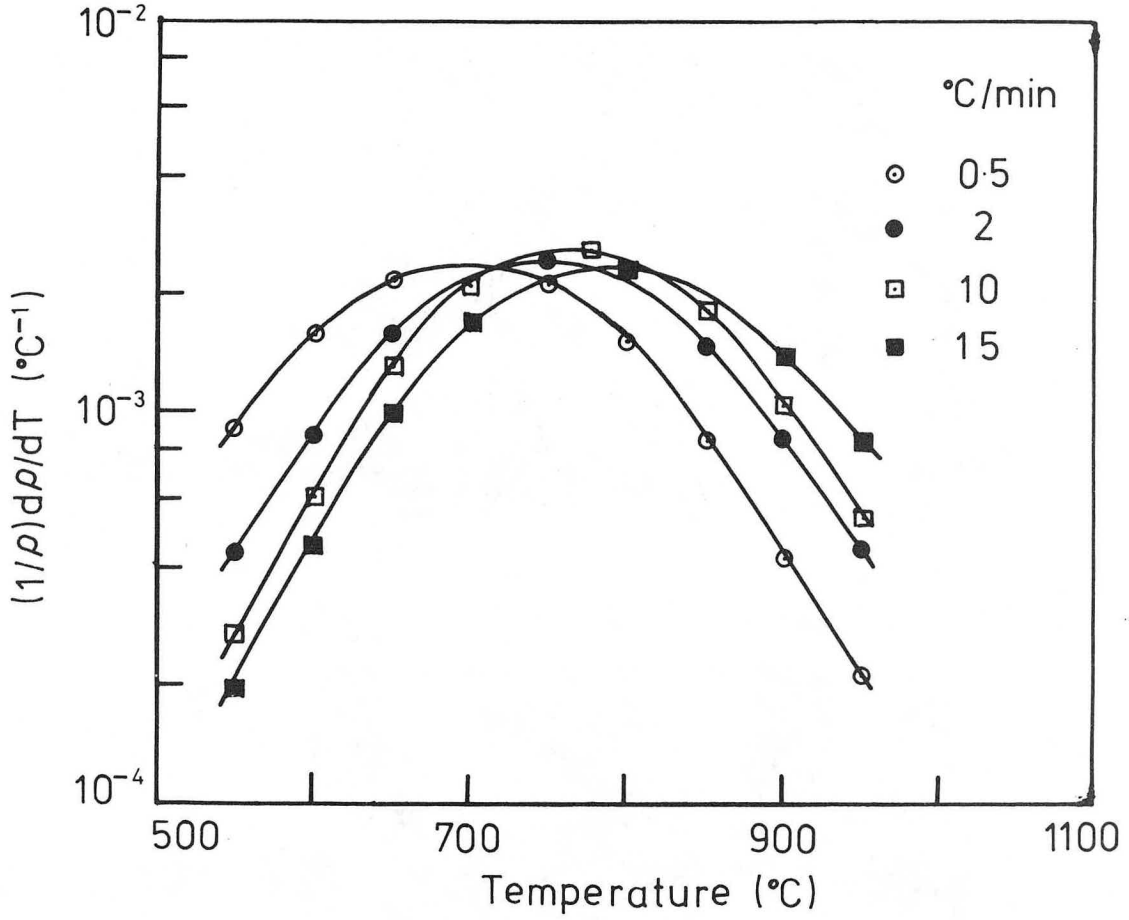

XBL 893-903

Figure 5

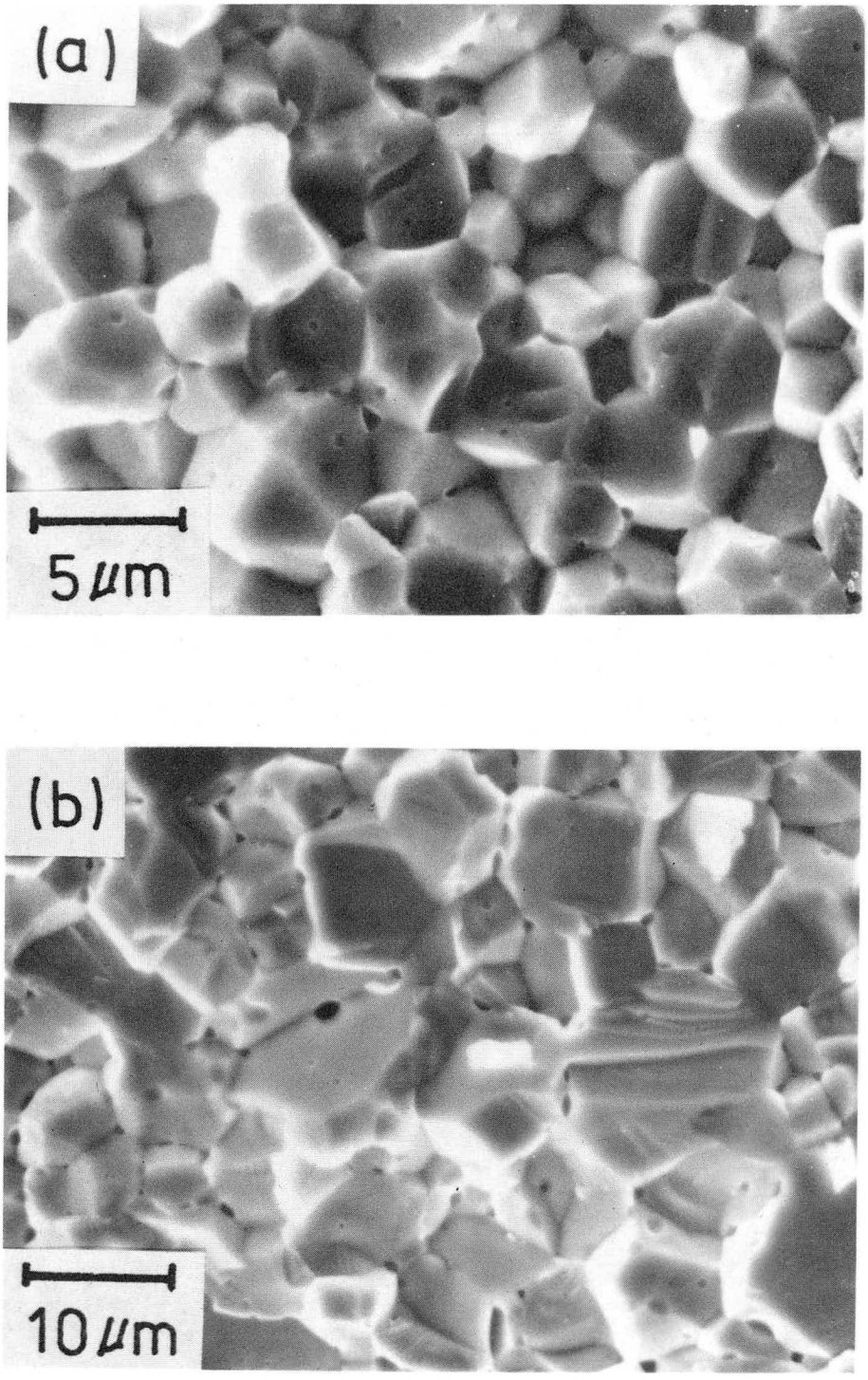

XBB. 893-1870A

Figure 6

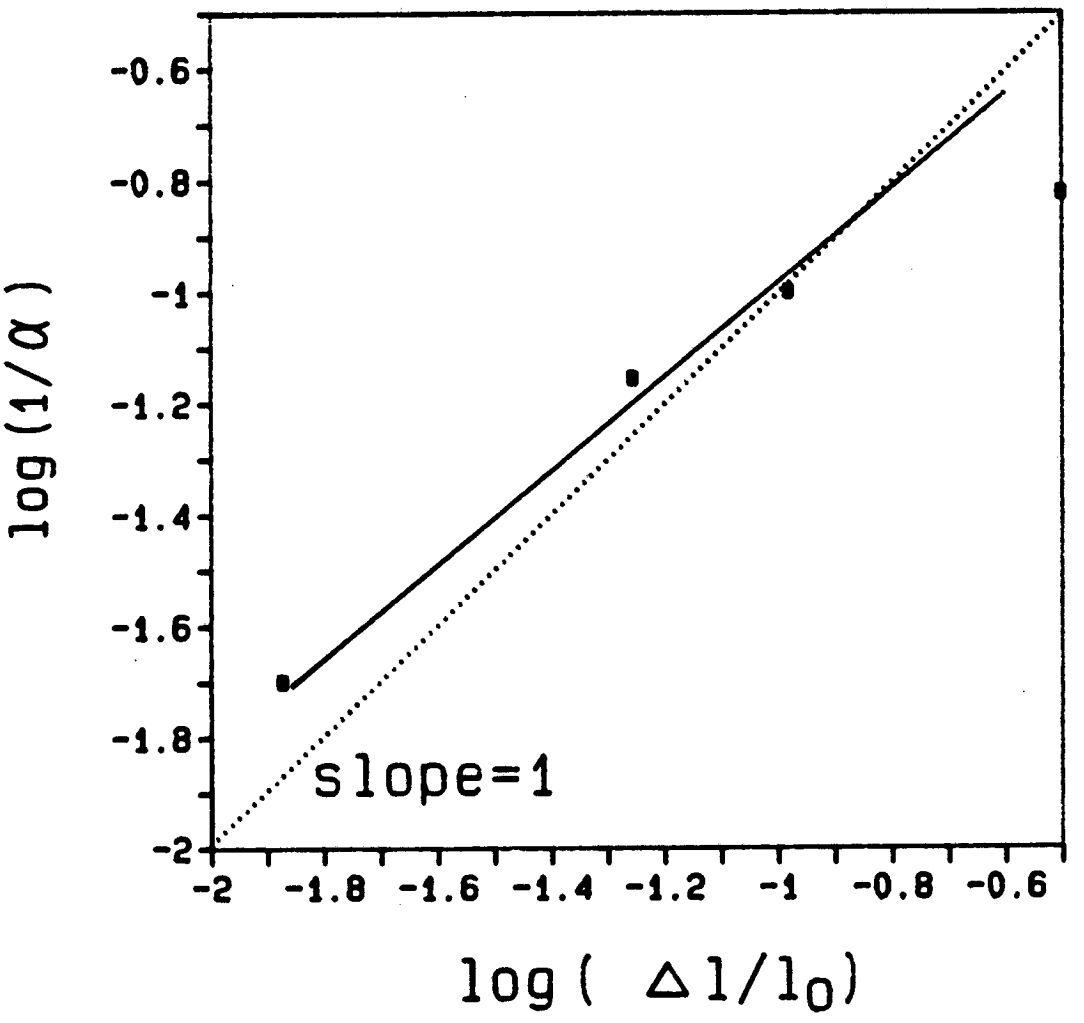
-0.6
-0.8
-1
-1.2
-1.4
-1.6
-1.8
-2
log(1/α)
slope=1
-2
-1.8
-1.6
-1.4
-1.2
-1
-0.8
-0.6
log(Δl/l0)
XBL 896-2385

Figure 7

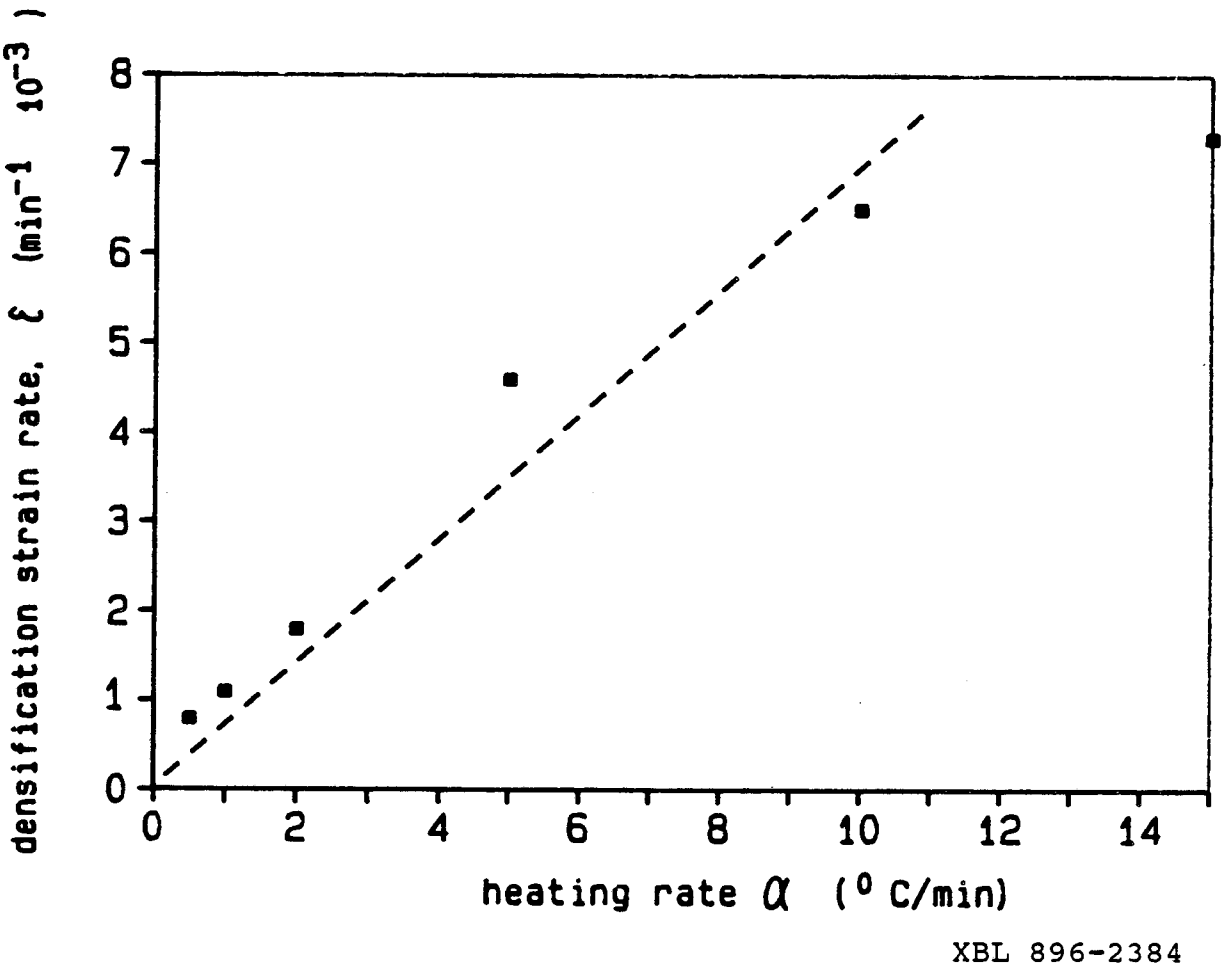
densification strain rate, $\dot{\varepsilon}$ (min^{-1} 10^{-3})
0
1
2
3
4
5
6
7
8
0
2
4
6
8
10
12
14
heating rate α (^{0} C/min)
XBL 896-2384

Figure 8

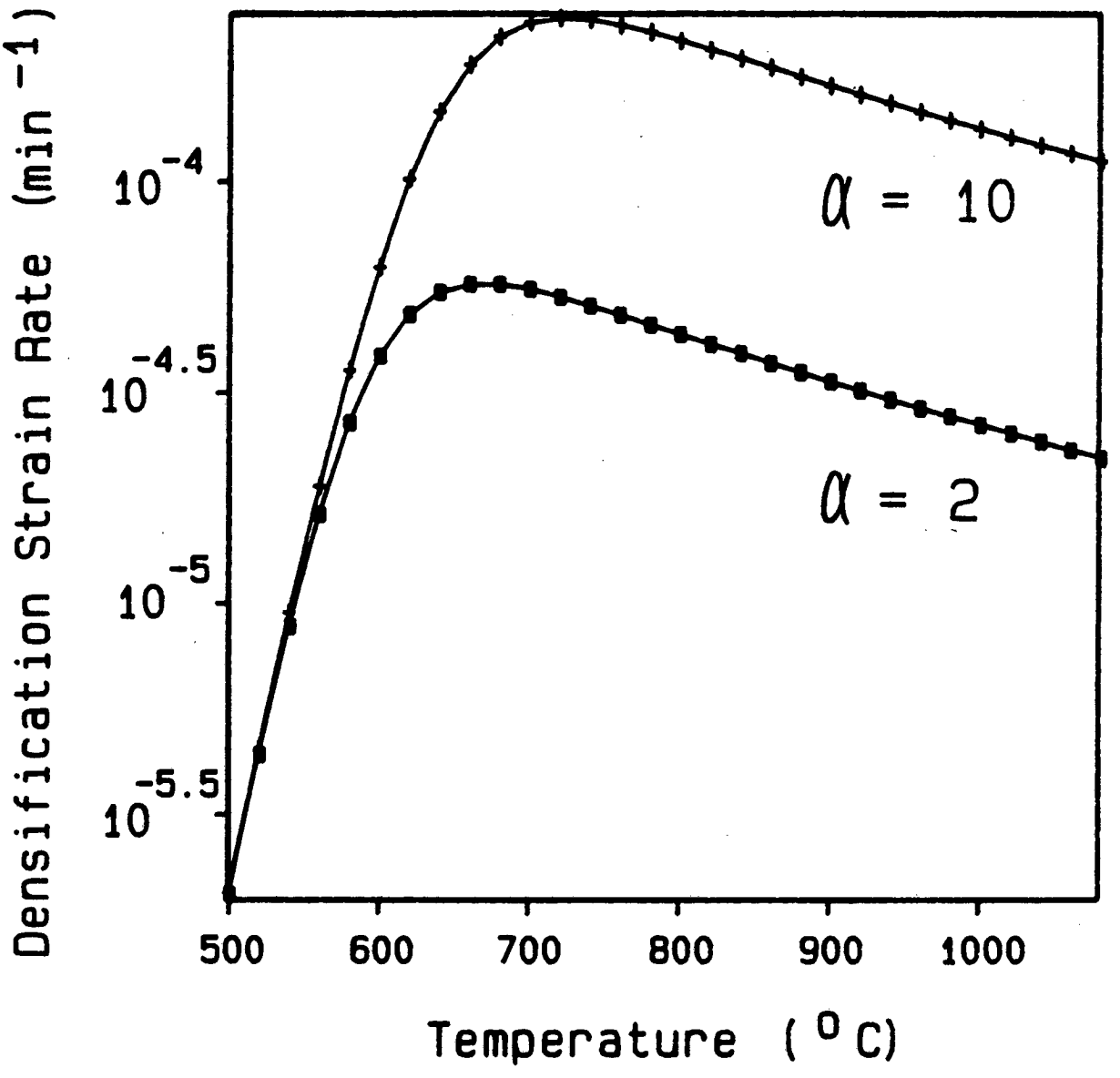

XBL 896-2382

Figure 9

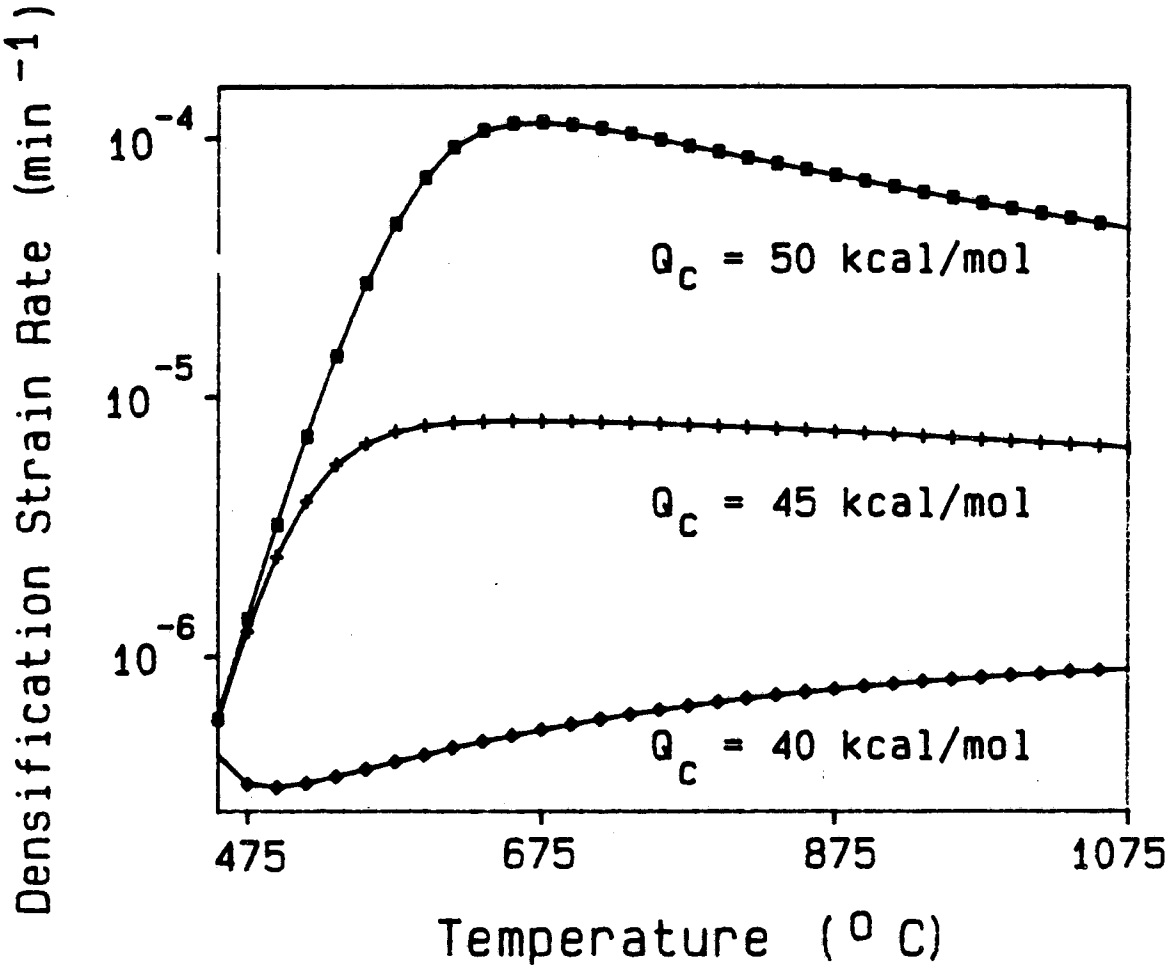

XBL 896-2383

Figure 10

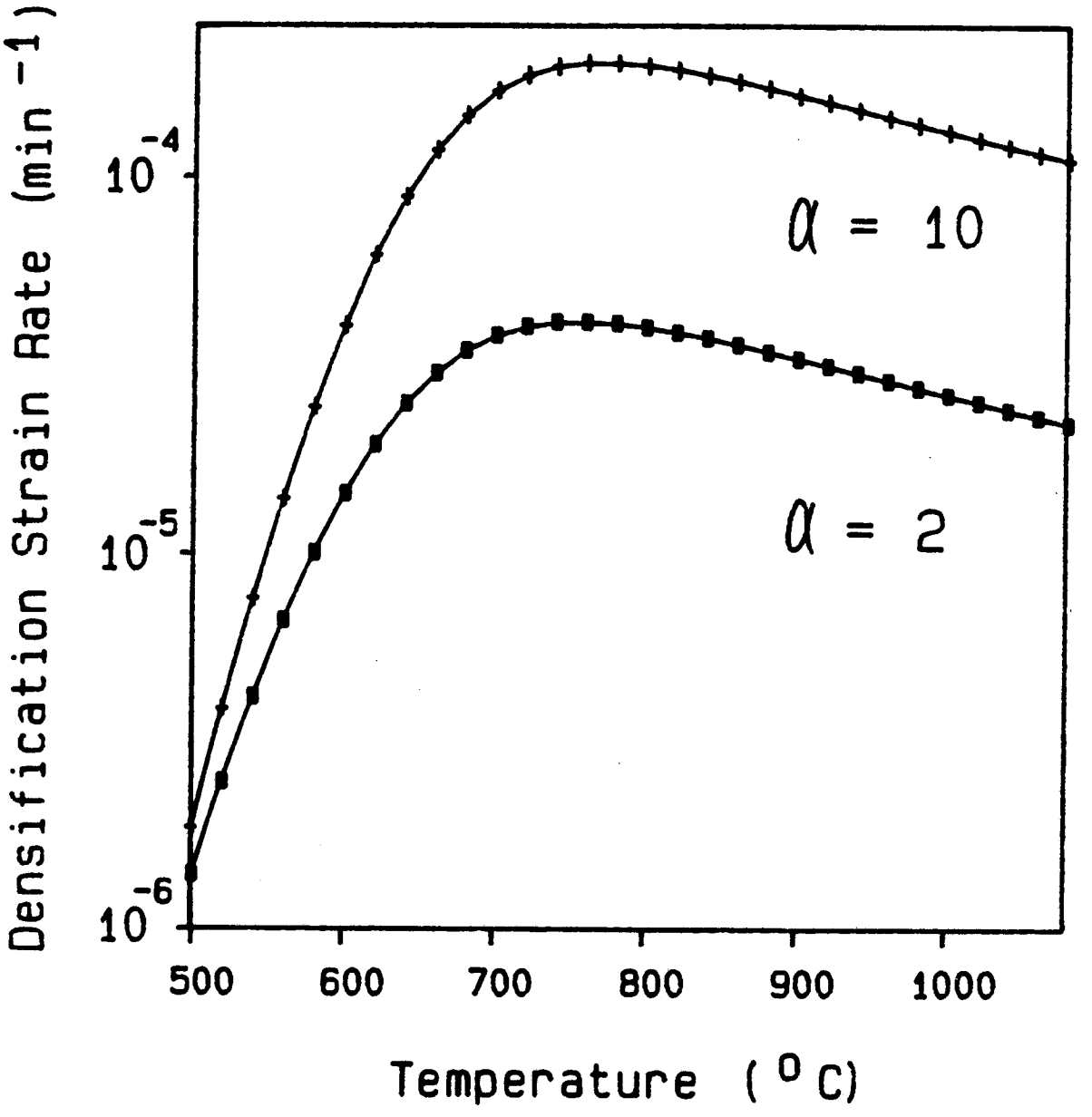

XBL 896-2381

Figure 11

LAWRENCE BERKELEY LABORATORY
CENTER FOR ADVANCED MATERIALS
1 CYCLOTRON ROAD
BERKELEY, CALIFORNIA 94720